Wavelet-sparsity based Regularization over Time in the Inverse Problem of Electrocardiography

Matthijs J. M. Cluitmans*†‡, Joël M. H. Karel*†, *Member, IEEE*, Pietro Bonizzi*†, *Member, IEEE*, Paul G. A. Volders‡, Ronald L. Westra†, Ralf L. M. Peeters†

***Abstract*— Noninvasive, detailed assessment of electrical cardiac activity at the level of the heart surface has the potential to revolutionize diagnostics and therapy of cardiac pathologies. Due to the requirement of noninvasiveness, body-surface potentials are measured and have to be projected back to the heart surface, yielding an ill-posed inverse problem. Ill-posedness ensures that there are non-unique solutions to this problem, resulting in a problem of choice. In the current paper, it is proposed to restrict this choice by requiring that the time series of reconstructed heart-surface potentials is sparse in the wavelet domain. A local search technique is introduced that pursues a sparse solution, using an orthogonal wavelet transform. Epicardial potentials reconstructed from this method are compared to those from existing methods, and validated with actual intracardiac recordings. The new technique improves the reconstructions in terms of smoothness and recovers physiologically meaningful details. Additionally, reconstruction of activation timing seems to be improved when pursuing sparsity of the reconstructed signals in the wavelet domain.**

I. INTRODUCTION

Heart rhythm disorders kill seven million people worldwide each year. Body-surface electrocardiograms (ECGs) are widely used to assess cardiac arrhythmias. However, these only reflect the attenuated and dispersed electromagnetic propagation of the hearts electrical activity to the body surface. Direct, noninvasive assessment of electrical processes at the level of the heart muscle would be of great benefit to clinical practice. This can be achieved by solving the inverse problem of electrocardiography, which would yield electrical intracardiac activity from body-surface ECGs and the corresponding patient-specific torso-heart geometry. During the last decades, much progress has been made in tackling the inverse problem of electrocardiography [1] and applications in humans appear with increasing frequency. [2] However, reconstruction of cardiac electrical activity remains imperfect. This is partly due to the ill-posedness of the inverse problem, meaning that little variation (noise) in the input data will yield large and unrealistic variations in the reconstructions. To cope with this problem, regularization is applied, incorporating additional constraints to arrive at more realistic solutions. Previously, we described the use of training data to improve reconstructions. [3] In this paper, we investigate the use of a novel reconstruction method that is based on constraints on the wavelet representation of the inverse problem solution. We will show that pursuing sparsity in the wavelet domain improves noninvasive reconstruction of electrical heart activity.

Human studies were approved by the Institutional Review Board at Maastricht University Medical Centre in Maastricht, the Netherlands, and informed consent was obtained from all patients. The study design, the data collection, the analysis and interpretation of data and the writing of the manuscript was done independently.

* Equally contributing authors.

† Joël Karel, Matthijs Cluitmans, Pietro Bonizzi, Ronald Westra and Ralf Peeters are with the Maastricht University Department of Knowledge Engineering, P.O. Box 616, 6200 MD Maastricht, The Netherlands Email: joel.karel@maastrichtuniversity.nl

‡ Matthijs Cluitmans and Paul Volders are with the Department of Cardiology, Cardiovascular Research Institute Maastricht (CARIM), Maastricht University Medical Centre, P.O. Box 5800, 6202 AZ Maastricht. Email: m.cluitmans@maastrichtuniversity.nl; Paul Volders was supported by The Netherlands Heart Foundation (NHS 2007T51).

II. THE INVERSE PROBLEM OF ELECTROCARDIOGRAPHY

The goal of the inverse problem of electrocardiography is to reconstruct electrical heart activity in terms of body-surface ECGs and the patient-specific geometry. The electrical activity of the heart can be represented by different models. Most often, models are chosen that reconstruct heart-surface potentials (epicardial potentials) or activation sequences. In this paper, we use a potential-based formulation. This is represented by the following forward problem:

$$\boldsymbol{A}\boldsymbol{Y}_{\mathrm{H}} = \boldsymbol{Y}_{\mathrm{B}} \tag{1}$$

in which $\boldsymbol{Y}_{\mathrm{B}}$ represents the vector of body-surface potentials, $\boldsymbol{Y}_{\mathrm{H}}$ is the vector of heart-surface potentials, and $\boldsymbol{A}$ is the transfer matrix that describes the electromagnetic relation between those potential vectors. The transfer matrix is based solely on geometrical and conductivity properties of the torso. Usually, the transfer matrix is determined from a patient-specific Computed Tomography (CT) scan. The inverse procedure is depicted in Fig. 1.

In the inverse problem, the body-surface potentials $\boldsymbol{Y}_{\mathrm{B}}$ and the transfer matrix $\boldsymbol{A}$ are assumed to be known. In reality, both are subject to uncertainty. The measured signal $\boldsymbol{Y}_{\mathrm{B}}$ is subject to noise and the matrix $\boldsymbol{A}$ is a mere estimate. Due to the ill-posedness of the problem, direct solutions are very sensitive to noise, even when $\boldsymbol{A}$ would be directly invertible. This generally is not possible, for example since it would require $\boldsymbol{Y}_{\mathrm{H}}$ and $\boldsymbol{Y}_{\mathrm{B}}$ to have the same number of mesh points, which usually is not the case. By applying regularization schemes, the ill-posed nature of this problem can be restricted. In this paper, we use the Generalized Minimal Residual (GMRes) method [4] as a comparison method, an application of iterative Krylov subspace methods. We compare this method to our new proposed setup. This new method is based on maximizing sparsity of the wavelet

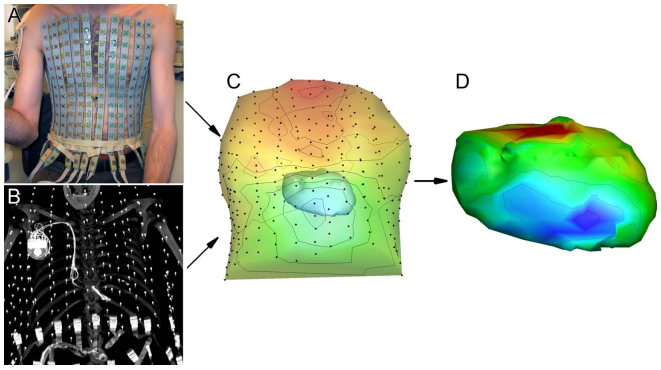

Fig. 1. The inverse procedure to reconstruct electrical heart activity noninvasively, as applied in the data collection for this paper. (A) Body-surface potentials $\boldsymbol{Y}_{\mathrm{B}}$ are obtained with an extensive set of electrodes (n=256) attached to the torso of the subject. (B) The location of the body-surface electrodes and of the outer heart surface is determined from a CT scan. (C) The heart-torso geometry can be coupled with the measured body-surface potentials. (D) By applying inverse algorithms, the corresponding electrical heart activity can be reconstructed. Note that this patient carried an implantable pacemaker (which can be seen in the CT scan), with leads in the left and right ventricle enabling recording of intracardiac potentials.

representation to obtain improved reconstructions of heart-surface potentials, similar to applications in tomographic inversion. [5]

III. SUBJECT AND MATERIALS

Test and validation data were obtained from a patient in the Maastricht University Medical Center (MUMC+, Maastricht, The Netherlands). Data collection consisted of three recordings: 1) Extensive body-surface potential recordings; 2) A computed tomography (CT) scan; 3) Intracardiac lead recordings. Body-surface potential (BSP) recordings were obtained with 256 electrodes attached to the torso of the patient. Recordings were taken for an extensive period, including native rhythm (with a left bundle branch block (LBBB) morphology), and pacing by implanted pacemaker. After body-surface potential recording, a CT scan was obtained with the electrodes still attached to the patient's torso. A geometry was created from the electrode positions (representing the body surface) and the outer heart surface. The conductor volume was assumed to be homogeneous. A transfer matrix relating the electrical activity at the heart surface to the body surface was computed with methods available from the SCIrun software repository. [6] A few months after this procedure, pseudo-unipolar electrograms were recorded with the implanted pacemaker from an epicardial lead in the left ventricle and an endocardial lead in the right ventricle. These recordings were obtained for a paced beat and a native beat. Although the recordings were not obtained simultaneously with the other data sets, the corresponding 12-lead ECG was equal for those beats. Therefore, these recordings could be used for validation purposes, although their pseudo-unipolar characteristics prevent exact morphological comparison to reconstructed unipolar electrograms.

The combination of body-surface potentials and geometry was used to reconstruct potentials at the heart surface. Validation of the reconstructed potentials was performed by comparing them to the heart-surface potentials recorded with the pacemaker leads. For the paced beats, additional validation was possible by comparing the reconstructed location of earliest activation with the known location of pacing.

The BSP recordings were band-pass filtered between [0.5,100]Hz (3rd order Chebyshev filter with stopband ripple of 20dB), to remove respiration related baseline wander and muscular artifacts, and notch filtered with cut-off frequency of 50Hz to remove powerline interference.

IV. METHODS

A. Iteration scheme

The inverse problem at hand is to determine the matrix $\boldsymbol{Y}_{\mathrm{H}}$ from (1), where $\boldsymbol{A}$ is the the $q \times p$ transfer matrix, $\boldsymbol{Y}_{\mathrm{H}}$ denoted the epicardial potentials and is an $p \times m$ matrix over p gridpoints over pseudospace and m samples over time, taking the role of $\boldsymbol{m}$ in [5]. The $q \times m$ matrix $\boldsymbol{Y}_{\mathrm{B}}$ is the matrix of body-surface potentials using a grid of q points and taking the role of $\boldsymbol{d}$ in [5]. Due to the topology of the heart and torso it is an open problem of how to take the wavelet transform over space in a meaningful way. Therefore, it was decided not to regularize by taking the wavelet transform over space as in [5], but to regularize over time. As a result the wavelet transform takes the form:

$$\boldsymbol{P} = \boldsymbol{Y}_{\mathrm{H}}\boldsymbol{W}^T \quad \text{and} \quad \boldsymbol{Y}_{\mathrm{H}} = \boldsymbol{P}\boldsymbol{W}$$

where $\boldsymbol{W}$ is the $m \times m$ orthogonal wavelet transform matrix. This choice differs from [5] such that $\boldsymbol{W}\boldsymbol{W}^T = \boldsymbol{W}^T\boldsymbol{W} = \boldsymbol{I}$. Consequently the functional [5, specifically their equation (1)] changes, taking the differences in notation and the change from vectors into matrices into account, to

$$\begin{aligned} \mathcal{I}_1(\boldsymbol{P}) &= \|\boldsymbol{Y}_{\mathrm{B}} - \boldsymbol{A}\boldsymbol{Y}_{\mathrm{H}}\|_F^2 + 2\tau\|\boldsymbol{P}\|_1 \qquad (2) \\ &= \|\boldsymbol{Y}_{\mathrm{B}} - \boldsymbol{A}\boldsymbol{P}\boldsymbol{W}\|_F^2 + 2\tau\|\boldsymbol{P}\|_1, \qquad (3) \end{aligned}$$

where $\|\cdot\|_F$ denote the Frobenius norm and $\|\cdot\|_1$ denotes the entrywise 1-norm. The surrogate function [5, Eq. (2)] changes to:

$$\mathcal{I}_1^{(n)}(\boldsymbol{P}) = \mathcal{I}_1(\boldsymbol{P}) - \|\boldsymbol{A}(\boldsymbol{P} - \boldsymbol{P}^{(n)})\boldsymbol{W}\|_F^2 + \|\boldsymbol{P} - \boldsymbol{P}^{(n)}\|_F^2. \qquad (4)$$

The surrogate function (4) can, for the purpose of minimization, be rewritten as:

$$\mathcal{I}_1^{(n)}(\boldsymbol{P}) = \|\boldsymbol{P} - (\boldsymbol{A}^T\boldsymbol{Y}_{\mathrm{B}}\boldsymbol{W}^T + (\boldsymbol{I} - \boldsymbol{A}^T\boldsymbol{A})\boldsymbol{P}^{(n)})\|_F^2 + 2\tau\|\boldsymbol{P}\|_1 + c^{(n)}, \qquad (5)$$

where $c^{(n)}$ does not depend on $\boldsymbol{P}$.

Since no mixing occurs with respect to $\boldsymbol{P}$, the derivative of (5) is given by

$$p_{i,j} - (\boldsymbol{A}^T\boldsymbol{Y}_{\mathrm{B}}\boldsymbol{W}^T + (\boldsymbol{I} - \boldsymbol{A}^T\boldsymbol{A})\boldsymbol{P}^{(n)})_{i,j} + \tau\,\mathrm{sign}(p_{i,j}) \qquad (6)$$

Similar to [5, Eq. (5)] the next iteration $\boldsymbol{P}^{(n+1)}$ is found by:

$$\boldsymbol{P}^{(n+1)} = \mathcal{S}_\tau\left[\boldsymbol{A}^T\boldsymbol{Y}_{\mathrm{B}}\boldsymbol{W}^T + (\boldsymbol{I} - \boldsymbol{A}^T\boldsymbol{A})\boldsymbol{P}^{(n)}\right], \qquad (7)$$

where $\mathcal{S}_\tau$ is the soft-thresholding [7] operation and τ is used as a (possibly scale dependent) threshold that will be applied

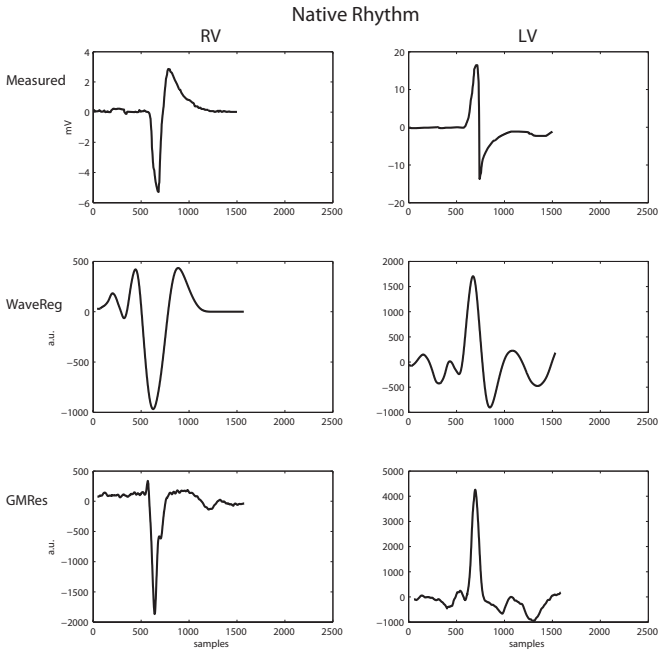

Fig. 2. LBBB native rhythm. First row: RV endocardial lead (left) and LV epicardial lead (right) measurements. Second row: RV (left) and LV (right) epicardial potentials reconstructed by wavelet-based regularization (WaveReg). Third row: RV (left) and LV (right) epicardial potentials reconstructed by GMRes; a.u.: arbitrary units.

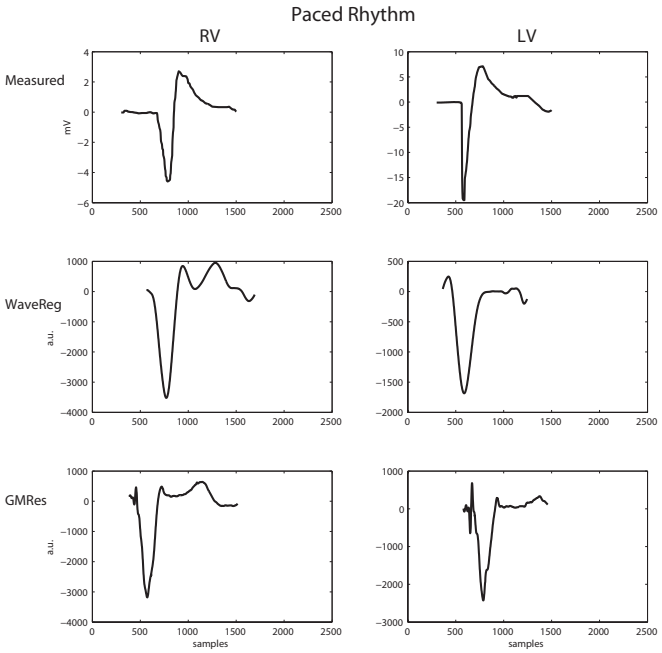

Fig. 3. Paced rhythm. Plots are as in Fig. 2

iteratively. Due to the iterative nature of this thresholding step, the choice of τ is not straightforward and should be much lower than the choice of threshold for a single thresholding step. Furthermore, the value of the threshold is dependent on the wavelet kernel at hand.

Due to the fact that the assumption is made that $\boldsymbol{W}$ is orthogonal, the wavelet employed can for e.g. be a Daubechies wavelet [8] or a wavelet that has been designed specifically for the signal at hand [9].

In [5] a number of recommendations are made such as rescaling the transfer matrix $\boldsymbol{A}$ and using a two-step procedure. These recommendations apply here as well, where the reader is cautioned that the parameter τ should change accordingly.

B. Starting point

The iteration scheme is a local search technique that is initialized from $\boldsymbol{P}^{(0)}$, and in general this search technique has the tendency to end in a local optimum. As a result a reasonable starting point $\boldsymbol{P}^{(0)}$ is essential. Taking merely the pseudoinverse of (1) will provide a noisy result for the problem at hand. Therefore the choice is made to start from a so-called "truncated SVD" (tSVD) solution. This initial solution is obtained as follows:

1) Compute the singular value decomposition (SVD) of the transfer matrix: $\boldsymbol{A} = \boldsymbol{U}\boldsymbol{D}\boldsymbol{V}^T$
2) Truncate the SVD to the b most significant components and reconstruct the SVD truncated transfer matrix $\widetilde{\boldsymbol{A}}$: $\widetilde{\boldsymbol{A}} = \boldsymbol{U}^{[b]}\boldsymbol{D}^{[b]}{\boldsymbol{V}^{[b]}}^T$, where $^{[b]}$ denotes the matrix has been truncated to its b most significant components
3) Compute $\boldsymbol{Y}_{\mathrm{H}}^{(0)}$ using the the pseudoinverse of the SVD truncated transfer matrix $\widetilde{\boldsymbol{A}}$: $\boldsymbol{Y}_{\mathrm{H}}^{(0)} = \widetilde{\boldsymbol{A}}^{\sharp}\boldsymbol{Y}_{\mathrm{B}}$
4) Obtain the actual starting point by taking the wavelet transform: $\boldsymbol{P}^{(0)} = \boldsymbol{Y}_{\mathrm{H}}^{(0)}\boldsymbol{W}^T$

The parameter b has a typical value of 20.

V. RESULTS

The approach was tested on a limited dataset consisting of a number of heart beats. Experiments show that the use of the Daubechies 8 wavelet (i.e. with 4 vanishing moments) gives a smoother solution than the use of the Daubechies 4 wavelet. Due to the uncertainty of the reconstruction the smoother solution was preferred and the choice was made to use the Daubechies 8 wavelet. The number of scales was chosen to be 7, such that all coefficients that correlate with a single beat appear in the detail coefficients. The parameter τ was set by experimentation and the recommendation from [5] was followed to use a threshold value for the approximation coefficients that is a factor 10 lower than for the detail coefficients. The implementation allows for using different thresholds for different scales for further fine-tuning. The results presented here have a threshold of 3.2 for the approximation coefficients and 32 for the detail coefficients, where note should be taken that the signal is rescaled by a factor α following the recommendations of [5], to have a matrix $\boldsymbol{A}$ that is scaled such that the largest eigenvalue of $\alpha^2\boldsymbol{A}^T\boldsymbol{A}$ is just below unity, ensuring faster convergence. The two-step iteration procedure from [5] was employed where each iteration step was performed 1000 times.

In Fig. 2, the reconstruction of a left bundle branch block beat is illustrated. The smoothness of the reconstruction has increased as desired and artifacts on the slopes have disappeared. For the right ventricular location the proposed

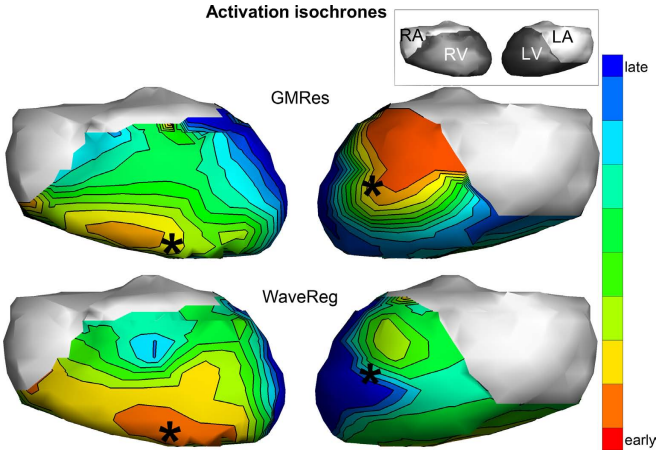

Fig. 4. Ventricular activation times of a paced heart beat. This beat developed after pacing on two different locations: first the right ventricle and 10ms later on the left ventricle. Asterisks indicate the location of the pacing leads. The top row shows the reconstructed activation times based on the GMRes reconstruction, the bottow row is based on the wavelet regularization. Red indicates early activation, blue indicates late activation. For a color figure, please refer to the online version of this paper.

reconstruction seems to also capture the positive deflection after the initial negative deflection, which traditional methods such as GMRes and tSVD were unable to reconstruct. Furthermore, in the left ventricle the negative deflection after the initial positive deflection is not captured by GMRes, but is apparent from the wavelet-sparsity based reconstruction. Of course, these results should be considered with care, as the intracardiac measurements date from several months after the BSP mapping, although the 12 lead ECG has been verified manually to ensure that similar signal morphology.

Fig. 3 illustrates the reconstruction of a paced beat. The wavelet-sparsity based reconstructions again seem to be closer in morphology to the measurements than the reference regularization method. For example, the positive deflection measured at the right ventricle after the initial negative deflection seems to be more pronounced with our proposed method. However, also a late deflection seems to be more pronounced. This deflection was already present in the starting point, which seems to indicate that the local search technique has not been able to move away far enough from this initial solution.

In Fig. 4 the timing of activation (defined as the maximum negative deflection of the reconstructed electrogram) is shown over the ventricular surface. The reconstructed locations of earliest activation should coincide with the pacing locations. The wavelet-based reconstruction fulfills this criterion better than the GMRes-based activation times. Moreover, the timing of activation (RV before LV) is in opposite order for the GMRes-based reconstruction, but in correct order for the wavelet-based reconstruction. Clearly, the wavelet-based approach performs better in this example.

Both Figs. 2 and 3 show unwanted oscillations in the reconstructed potentials. Another choice of wavelet type and threshold level might yield improved results. However, even with these oscillations present, major physiological parameters (such as activation times) seem to be intact or even improved when compared to traditional reconstruction methods.

VI. DISCUSSION

We have shown that wavelet-based sparsity reconstruction of epicardial potentials is feasible and yields results that are equal to or even better than existing reconstruction methods. The restriction of wavelet sparsity limits the solution space, thereby reducing the influence of ill-posedness on the reconstructed signals. The current choice for the Daubechies 8 wavelet ensures smoothness, but other choices of orthogonal wavelets can enforce other desirable properties of reconstructions. The quality of the reconstructions is also dependent on the starting point. With an inconvenient starting point, the optimization might terminate in a solution that contains waves that are not present in the actual signal. Since the transfer matrix and the BSPs are both subject to uncertainty it is recommended that as much patient-specific information as possible is included in the starting point to ensure that the amount of uncertainty is reduced.

The propagation of electrical potentials over the heart surface is obviously also dependent on spatial characteristics. Future improvements would aim at coupling the wavelet representation of these signals not only over time but also over space. This would require a wavelet transform that decomposes the local electrograms on a heart surface over time; i.e. in three dimensions, where the surface is not in a plane, but takes the geometry of the heart. How to construct such wavelet transform is yet an open question but would improve the initials results presented in this paper even further.

REFERENCES

[1] R. S. MacLeod and D. H. Brooks. Recent progress in inverse problems in electrocardiology. *IEEE Eng Med Biol Mag*, 17(1):73–83, 1998.

[2] C. Ramanathan, R. N. Ghanem, K. Ryu P. Jia, and Y. Rudy. Noninvasive electrocardiographic imaging for cardiac electrophysiology and arrhythmia. *Nat Med*, 10(4):422–428, 2004.

[3] Matthijs Cluitmans, Ralf Peeters, Paul Volders, and Ronald Westra. Realistic training data improve noninvasive reconstruction of heart-surface potentials. In *Conf Proc IEEE Eng Med Biol Soc*, pages 6373–6376, 2012.

[4] C. Ramanathan, P. Jia, R. Ghanem, D. Calvetti, and Y. Rudy. Noninvasive electrocardiographic imaging (ECGI): application of the generalized minimal residual (GMRes) method. *Ann Biomed Eng*, 31(8):981–994, 2003.

[5] Ignace Loris, Guus Nolet, Ingrid Daubechies, and F.A. Dahlen. Tomographic inversion using ℓ_1-norm regularization of wavelet coefficients. *Int. J. Geophys.*, 170:359–363, 2007.

[6] Brett M Burton, Jess D Tate, Burak Erem, Darrell J Swenson, Dafang F Wang, Michael Steffen, Dana H Brooks, Peter M van Dam, and Rob S Macleod. A toolkit for forward/inverse problems in electrocardiography within the SCIrun problem solving environment. In *Conf Proc IEEE Eng Med Biol Soc*, pages 267–270, 2011.

[7] David L. Donaho. De-noising by soft-thresholding. *IEEE Trans. Inform. Theory*, 4(3):613–627, 1995.

[8] I. Daubechies. Orthonormal bases of compactly supported wavelets, II. variations on a theme. *SIAM J. Math. Anal.*, 24(2):499–519, 1993.

[9] J.M.H. Karel, R.L.M. Peeters, R.L. Westra, K. Moermans, S.A.P. Haddad, and W.A. Serdijn. Optimal discrete wavelet design for cardiac signal processing. In *Conf Proc IEEE Eng Med Biol Soc*, pages 2769–2772, 2005.